

Supporting Information

Rational design of high performance nanotheranostics for NIR-II fluorescence/magnetic resonance imaging guided enhanced phototherapy

Qi Wang ^{a,b}, Jie Cai ^a, Xinrui Niu ^a, Jing Wang ^a, Jiawei Liu ^a, Chen Xie ^{a,*}, Wei
Huang ^a, Quli Fan ^{a,*}

*^a Key Laboratory for Organic Electronics and Information Displays & Jiangsu Key
Laboratory for Biosensors, Institute of Advanced Materials (IAM), Jiangsu National
Synergetic Innovation Center for Advanced Materials (SICAM), Nanjing University of
Posts & Telecommunications, Nanjing 210023, China*

E-mail: iamcxie@njupt.edu.cn; iamqlfan@njupt.edu.cn

*^b State Key Laboratory of Bioelectronics, Southeast University, Nanjing 210096,
China*

Table of Contents

1. <i>Materials and apparatus</i>	S3
2. <i>Synthesis of DPPB</i>	S3
3. <i>Molar absorption coefficient of DPPB-Gd-I NPs</i>	S5
4. <i>Photodynamic measurement of DPPB-Gd-I NPs</i>	S5
5. <i>Infrared thermal images of DPPB-Gd-I NPs</i>	S6
6. <i>Photothermal measurement of DPPB-Gd NPs</i>	S6
7. <i>Cellular uptake of NPs</i>	S7
8. <i>Penetration depth measurement of DPPB-Gd-I NPs</i>	S7
9. <i>Ex vivo NIR-II fluorescence imaging of tumor and major organs</i>	S7
10. <i>H&E stained images of tumor</i>	S8

1. Materials and apparatus

The Gd-DTPA-SA^[S1] and PEG-PHEMA-I^[S2] were prepared according to previous protocols. Calcein AM/PI stain kit, NIH-3T3 normal cells and HeLa cells were purchased from Nanjing KeyGEN Biotech. Co. Ltd. Other Chemicals were purchased from Aladdin. All mice studies were approved by Animal Ethics Committee of Nanjing KeyGEN Biotech. Co. Ltd. and performed in Nanjing KeyGEN Biotech. Co. Ltd. The morphology and size of NPs were determined by a HT7700 transmission electron microscope (TEM) and a particle size analyzer (Brookhaven Instruments), respectively. Absorption and emission spectra were obtained using a UV3600 UV/vis/NIR spectrophotometer (Shimadzu) and a FLSP920 fluorescence spectrophotometer (Edinburgh), respectively. The MTT experiments were conducted using a PowerWave XS/XS2 microplate reader (BioTek).

2. Synthesis of DPPB

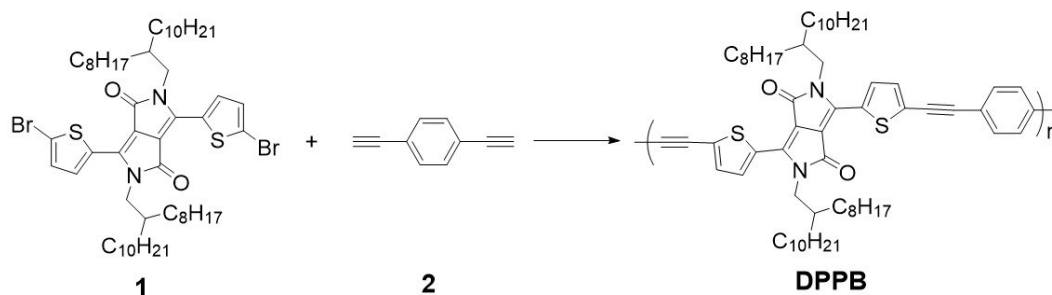


Fig. S1. Synthetic route of DPPB.

Compound **1** (0.1 mmol, 121 mg) and compound **2** (0.1mmol, 15 mg), Pd(PPh₃)₄ (15 mg), and diisopropylamine (30 mL) were mixed in a reaction bottle under N₂ atmosphere. The mixture was vigorously stirred at 85 °C for 48 h. After removal of the solvent, the crude product was settled with ether to obtain DPPB as a black-green solid.

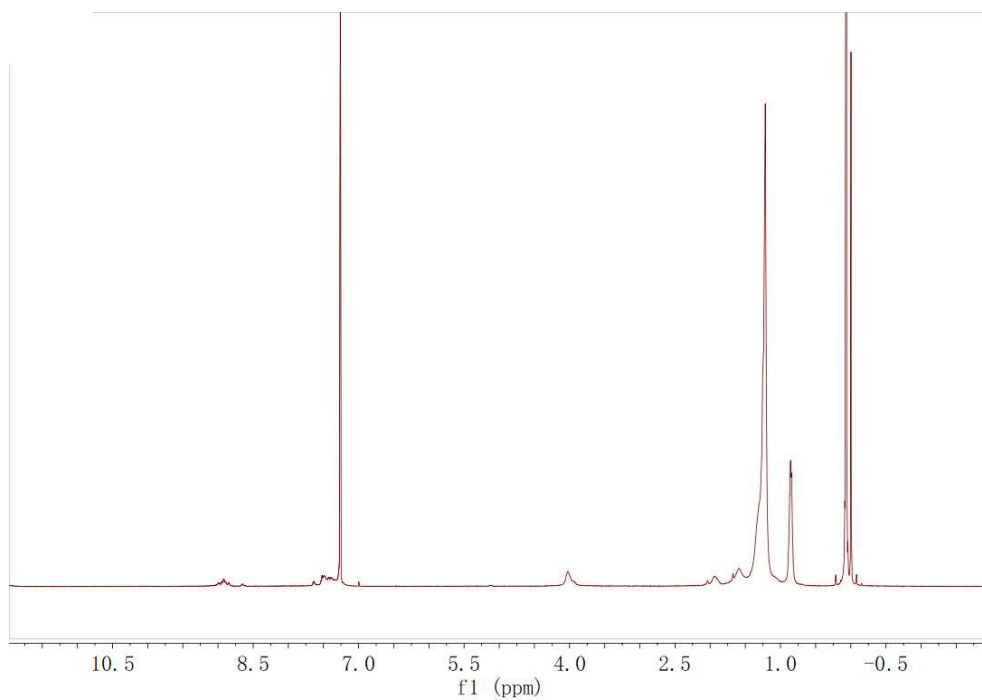


Fig. S2. ^1H NMR spectrum of DPPB.

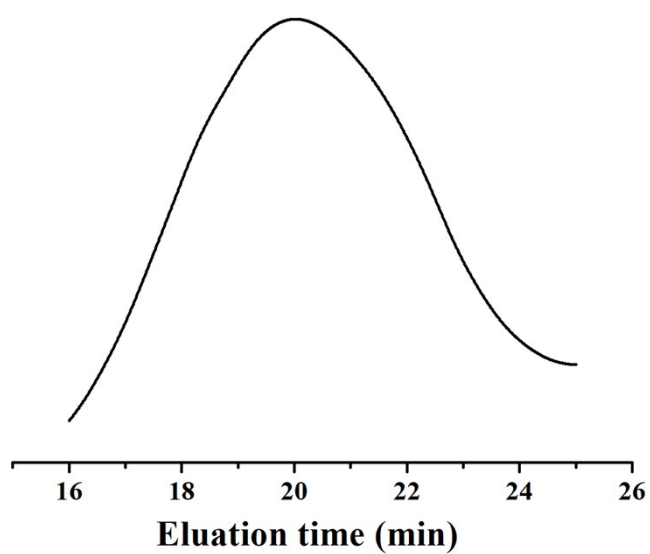


Fig. S3. GPC of DPPB, the number-average of DPPB was 14000.

3. Molar absorption coefficient of DPPB-Gd-I NPs

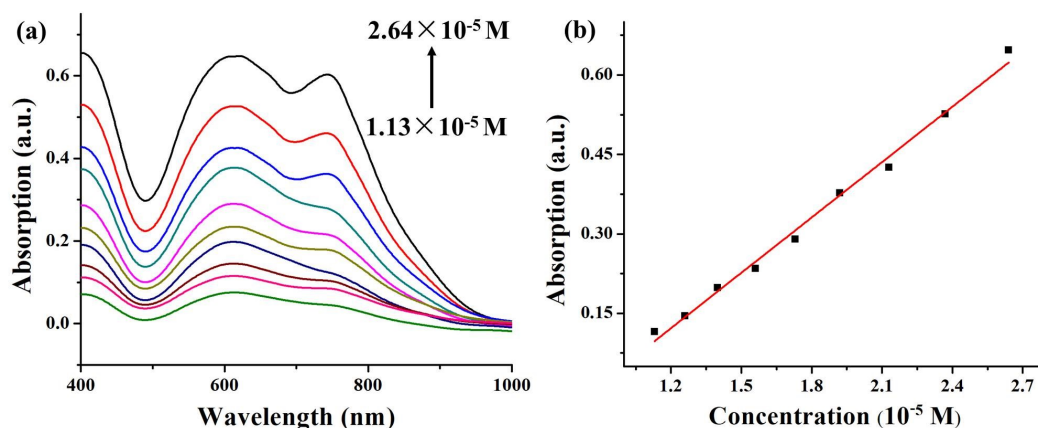


Fig. S4. (a) Absorption curves of DPPB-Gd-I NPs aqueous solution at different concentrations. (b) Linear absorbance versus concentration obtained from (a).

4. Photodynamic measurement of DPPB-Gd-I NPs

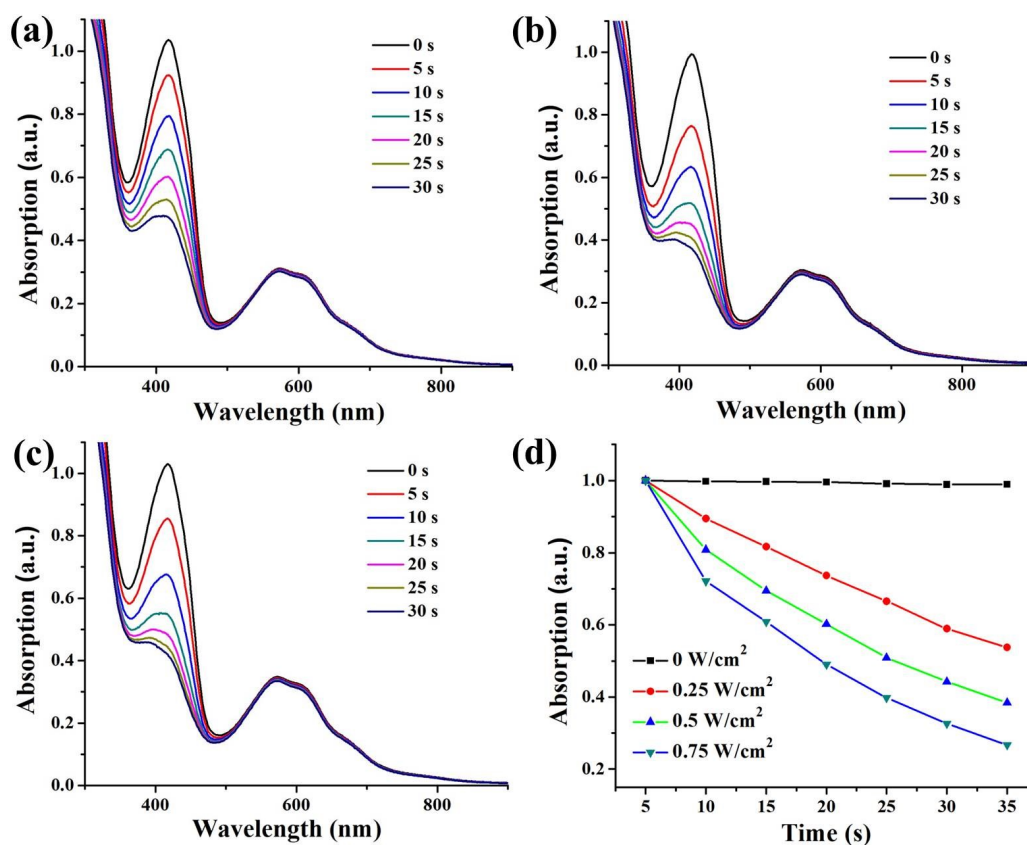


Fig. S5. Absorption spectra of the mixed aqueous solution of DPPB-Gd-I NPs and DPBF under 660 nm laser irradiation with different power densities (a) 0.25, (b) 0.50, (c) 0.75 W/cm². (d) The decline of normalized absorption of DPBF resulted from 660 nm light induced DPPB-Gd-I NPs.

5. Infrared thermal images of DPPB-Gd-I NPs

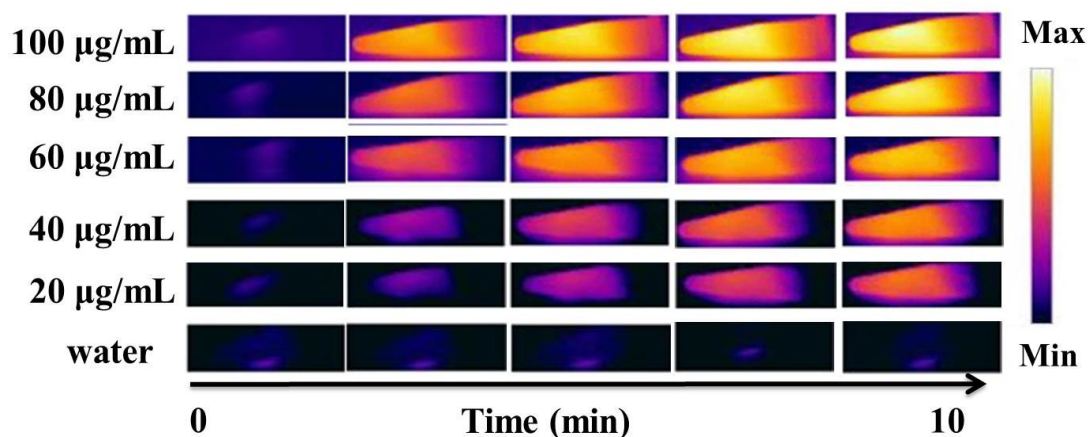


Fig. S6. (a) Infrared thermal images of DPPB-Gd-I NPs at various concentrations upon 660 nm laser illumination.

6. Photothermal measurement of DPPB-Gd NPs

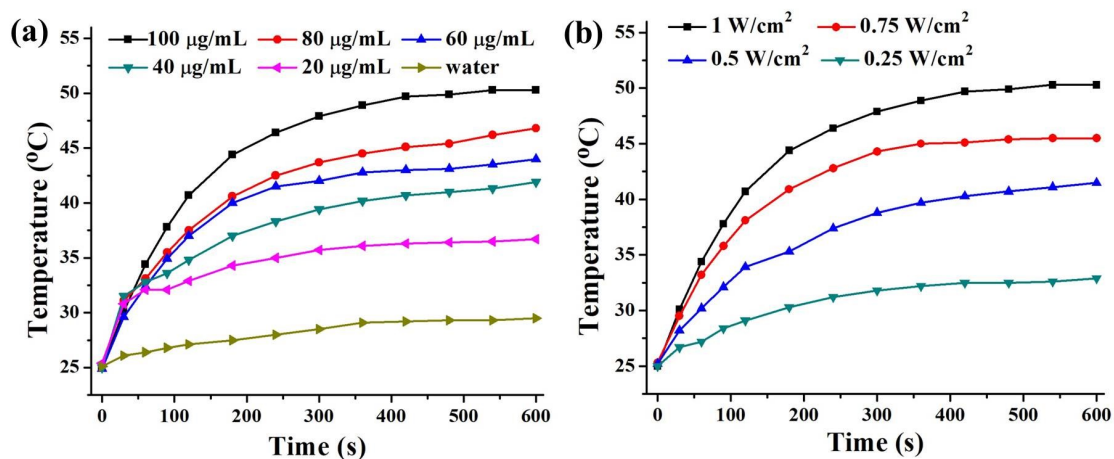


Fig. S7. (a) Heating curves of DPPB-Gd NPs at various concentrations upon 660 nm laser illumination. (b) Heating curves of DPPB-Gd NPs upon 660 nm laser illumination with various powers.

7. Cellular uptake of NPs

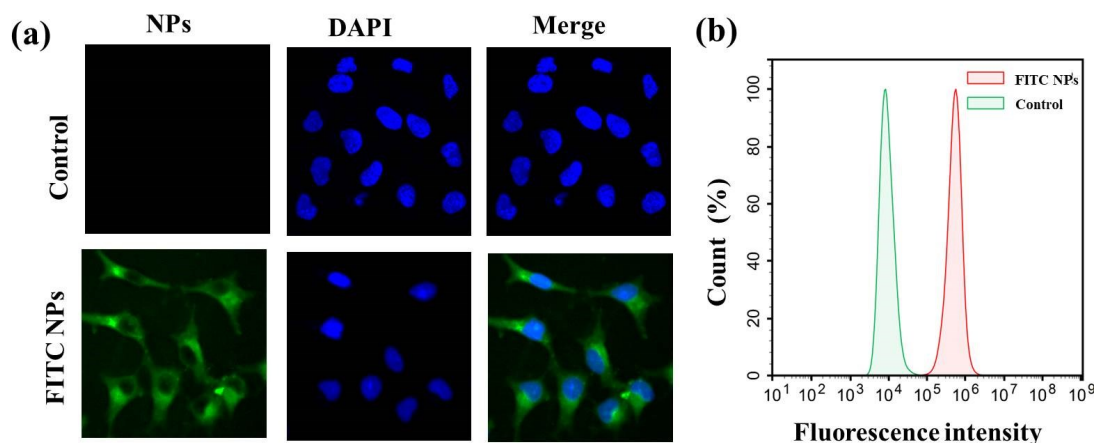


Fig. S8. The cellular uptake of NPs toward HeLa cells evaluated by (a) confocal laser scanning microscopy and (b) flow cytometry.

Due to the fluorescence emission wavelength of polymer was too long, which was not suitable for confocal laser scanning microscopy. Fluorescein isothiocyanate (FITC) was used as a model dye and encapsulated by Gd-DTPA-SA and PEG-PHEMA-I to form water-soluble FITC NPs. HeLa cells after incubation with FITC NPs for 12 h showed intense green fluorescence assigned to nanoparticles, indicating the effective cellular internalization of the NPs, which was consistent with the result of flow cytometry.

8. Penetration depth measurement of DPPB-Gd-I NPs

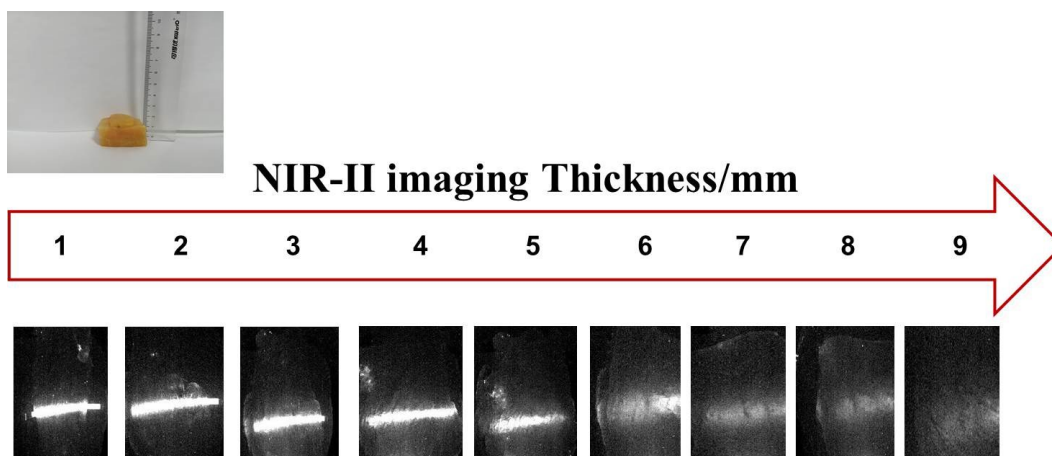


Fig. S9. Penetration depth measurement of DPPB-Gd-I NPs in a simulated deep-tissue setting (chicken-breast tissues).

9. Ex vivo NIR-II fluorescence imaging of tumor and major organs

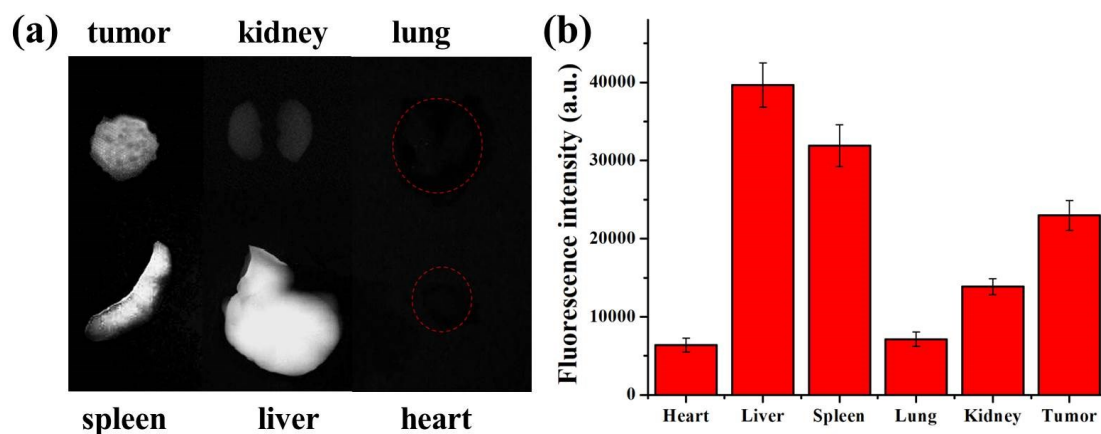


Fig. S10. (a) Ex vivo NIR-II image of tumors and major organs. (b) Semi-quantitative biodistribution analysis based on fluorescence intensity of tumors and major organs.

10. H&E stained images of tumor

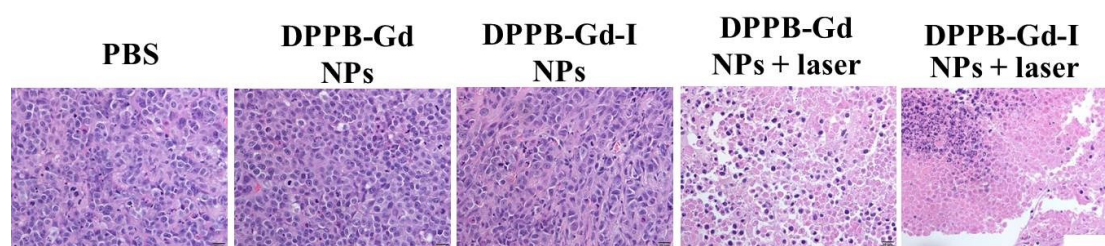


Fig. S11. H&E stained images of tumor. Scale bars: 80 μm .

References:

- [S1] Y. Dai, J. Su, K. Wu, W. Ma, B. Wang, M. Li, P. Sun, Q. Shen, Q. Wang, Q. Fan, Multifunctional thermosensitive liposomes based on natural phase-change material: near-infrared light-triggered drug release and multimodal imaging-guided cancer combination therapy, *ACS Appl. Mater. Interfaces* 11 (2019) 10540-10553.
- [S2] W. Zhou, Y. Chen, Y. Zhang, X. Xin, R. Li, C. Xie, and Q. Fan, Iodine-rich semiconducting polymer nanoparticles for CT/fluorescence dual-modal imaging-guided enhanced photodynamic therapy, *Small* 16 (2020) 1905641.